PHYSICAL REVIEW B VOLUME 53, NUMBER 13 1 APRIL 1996-I

Branching ratio of uv and blue upconversions of Tm^{3+} ions in glasses

Setsuhisa Tanabe
Department of Materials Chemistry, Faculty of Integrated Studies, Kyoto University, Sakyo-ku, Kyoto 606-01, Japan

Kiyoshi Tamai, Kazuyuki Hirao, and Naohiro Soga
Department of Materials Chemistry, Faculty of Engineering, Kyoto University, Sakyo-ku, Kyoto 606-01, Japan

(Received 15 November 1995)

Tm^{3+} doped germanate, tellurite and heavy-metal fluoride glasses were prepared and their upconversion luminescence spectra were measured to investigate the effect of the host glass on the branching ratios, β of ${}^1D_2 \rightarrow {}^3H_6$ at 0.36 μm and ${}^1D_2 \rightarrow {}^3F_4$ at 0.45 μm. Because the radiative emission probabilities of these electric dipole transitions are functions of Judd-Ofelt intensity parameters Ω_t and the sets of reduced matrix elements $\langle \| U^{(t)} \| \rangle (t=2,4,6)$, it was possible to vary the β of both transitions. The β of 0.45 μm luminescence increases slightly with increasing Ω_2 parameter, whereas β of 0.36 μm decreased. The ratio of β_{36}/β_{45} was largest in a fluorozincate glass and lowest in a tellurite glass. The result could be well explained by the smaller Ω_2/Ω_4 ratio in fluoride glasses than those in oxide glasses. The correlation between the luminescence intensity ratio and the Ω_t parameters shows that we can control the branching ratio by the ligand field design for Tm^{3+} in glass matrices.

I. INTRODUCTION

Solid state compact blue laser materials are required for higher density in the optical data storage as well as for multicolorization of visible lasers. The frequency upconversion by a Tm^{3+} doped fiber[1] has the possibility of a III-V semiconductor (AlGaInP, ~0.65 μm) laser pumped blue laser without the need of phase matching, which is necessary for second harmonic generation (SHG) by anisotropic nonlinear optical crystals. The glass hosts are attractive materials because they can be fabricated as optical waveguide structures like a fiber in which the pumping light can be confined efficiently to maintain a high intensity over a long interaction length. The upconversion lasing at 451 nm has already been attained in a fluorozirconate glass fiber by copumping at 676.4 and 647.1 nm of a krypton ion laser.[2] By investigating the dependence of upconversion efficiency on excitation wavelengths of a tunable dye laser, we provided evidence of the excited state absorption (ESA) mechanisms for Tm^{3+} upconversion shown in Fig. 1.[3] It is well known that Tm^{3+}: ${}^1D_2$ level has two intense transitions to ${}^3H_6$ and ${}^3F_4$ levels, the wavelengths of which are near 360 and 450 nm, respectively. The branching ratio, β for both transitions from ${}^1D_2$ in a fluoride glass were around 40% and 45%, respectively.[4] To attain efficient upconversion lasing, it is desirable to obtain single line by raising the β of only one of ${}^1D_2 \rightarrow {}^3H_6$ and ${}^1D_2 \rightarrow {}^3F_4$ transitions. The emission probability of electric dipole transitions is dominated by the Judd-Ofelt Ω_t parameters, which are functions of crystal field and radial integral of 4f and 5d electrons. The line strength of a transition between an initial $|aJ\rangle$ and final $|bJ'\rangle$ manifold is given by[5,6]

$$S[aJ;bJ'] = \sum_{t=2,4,6} \Omega_t \langle aJ \| U^{(t)} \| bJ' \rangle^2, \tag{1}$$

where $\langle aJ \| U^{(t)} \| bJ' \rangle$'s denote the reduced matrix elements of unit tensor operators for the corresponding transition. It is to be noted that the sets of reduced matrix elements of unit tensor operator, $U^{(t)}$ (Ref. 7) of them ($t=2,4,6$) have different features as shown in Table I; $\langle f^{12}\, {}^1D_2 \| U^{(2)} \| f^{12}\, {}^3H_6 \rangle^2$ is zero, while $\langle f^{12}\, {}^1D_2 \| U^{(2)} \| f^{12}\, {}^3F_4 \rangle^2$ is the largest among three. Thus it is expected that β of 450 nm emission can be gained by enhancing Ω_2 parameter of Tm^{3+}, whereas β of 360 nm can be by Ω_4.

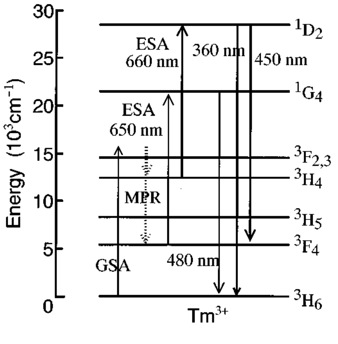

FIG. 1. Energy level and upconversion mechanisms of Tm^{3+} by excited state absorption.

Although there have been few reports on the controlling factors of Ω_t parameters, it has been in own semiempirically that the value of Ω_2 is raised drastically by lowering the symmetry of rare earth ligand field.[8,9] On the other hand, the

TABLE I. Reduced matrix elements $\langle f^{12}(SL)J \| U^{(t)} \| f^{12}(S'L')J' \rangle^2$ of radiative transitions from ${}^1D_2$ level. (See Ref. 7.) Typical wavelengths are included.

$(SL)J$	$(S'L')J'$	$[U^{(2)}]^{(2)}$	$[U^{(4)}]^{(2)}$	$[U^{(6)}]^2$	λ(μm)
${}^1D_2$	${}^3H_6$	0.0	0.3133	0.0934	0.36
	${}^3F_4$	0.5792	0.0968	0.0194	0.45
	${}^3H_5$	0.0	0.0017	0.0164	0.50

0163-1829/96/53(13)/8358(5)/$10.00

controlling factors of $\Omega_{4,6}$ have not yet clarified before we have shown the simple correlation between the Mössbauer isomer shift and Ω_6 in all kinds of glasses.[10] The $\Omega_{4,6}$ can be gained by lowering the covalency of σ-chemical bond between rare earth ion and ligand anions.[11] One way to obtain a large Ω_2 is to design an asymmetric field by changing the host matrix for the rare earth site.[10] In this study, Tm^{3+} upconversion characteristics in several heavy metal fluoride and oxide glasses and the effect of composition were investigated on Judd-Ofelt Ω_t parameters, and on the branching ratio of these ultraviolet and blue emissions.

II. EXPERIMENT

A. Sample preparation

The glass compositions employed are listed below:

ZnABSY: $40ZnF_2 \cdot 15AlF_3 \cdot 15BaF_2 \cdot 15SrF_2 \cdot 15YF_3 \cdot 0.1TmF_3$,
AlBCY: $40AlF_3 \cdot 22BaF_2 \cdot 22CaF_2 \cdot 16YF_3 \cdot 0.1TmF_3$,
ZrBL: $60ZrF_4 \cdot 33BaF_2 \cdot 7LaF_3 \cdot 0.1TmF_3$,
HfBL: $60HfF_4 \cdot 33BaF_2 \cdot 7LaF_3 \cdot 0.1TmF_3$,
TeBZ: $60TeO_2 \cdot 30BaO \cdot 10ZnO \cdot 0.1TmO_{1.5}$,
GeBZ: $60GeO_2 \cdot 30BaO \cdot 10ZnO \cdot 0.1TmO_{1.5}$.

High purity reagents were used as raw materials in preparing the glasses. The glasses obtained were annealed at the respective glass transition temperatures determined by a differential thermal analysis. The annealed samples were cut and polished into the shape of 5×5×1.5 mm^3.

B. Absorption spectra and Judd-Ofelt analysis

Absorption spectrum was measured with a Shimadzu UV-3101PC Recording Spectrophotometer in the wavelength range of 300–2200 nm. The density of the samples were measured by Archimedes method using kerosene as the immersing liquid and a silica glass as a standard. From the molecular weight and measured density, the Tm^{3+} concentration, ρ_N was calculated. The refractive index, n of the glass was measured with an ERMA Abbe refractometer. From the integrated absorbance, three intensity parameters Ω_t ($t=2,4,6$) were determined as follows.

The line strength of an absorption band between an initial J manifold $|aJ\rangle$ and final manifold $|bJ'\rangle$, $S_{JJ'}$ was calculated with the experimental values of the integrated absorbance by[9]

$$\int_{\text{band}} k(\lambda)\,d\lambda = \frac{8\pi^3 e^2 \lambda_m \rho_N}{3hc(2J+1)} \frac{1}{n} \left[\frac{(n^2+2)^2}{9} \right] S_{JJ'}, \qquad (2)$$

where $k(\lambda)$ is the absorption coefficient at λ, λ_m is the mean wavelength of the absorption band determined as the center of gravity, h is Planck's constant, c is the speed of light, and e is the elementary charge. Thus a least square fitting approach was done with the data of ρ_N, n, integrated absorbance and sets of $\langle \| U^{(t)} \| \rangle^2$ (Ref. 5) of 4 bands ($^3H_4$, $^3F_{2,3}$, $^1G_4$, and $^1D_2 \leftarrow {}^3H_6$) to obtain three intensity parameters Ω_t ($t=2,4,6$) by using Eqs. (1) and (2).

C. Luminescence measurement

The luminescence and excitation spectra were measured with a Hitachi-850 Fluorescence Spectrophotometer. For the phonon sideband measurement, as closed-cycle helium refrigerator (Iwatani CRT-006-2000) was used to keep the temperature of 12 K and the internal xenon lamp was used as an excitation source. A dye laser (Spectra Physics Model 375B Dye Laser) excited by a cw Ar^+ laser (Coherent innova 70) was used as a pumping source for upconversion luminescence. A propylene carbonate solution of DCM dye (dicyanomethylene-2-methyl-6-p-dimethylaminostyryl-4H-pyran) was used to obtain tunable range of 630–680 nm.

TABLE II. The Ω_t parameters of Tm^{3+} ions in the glasses.

Glass	Ω_2	Ω_4 (10^{-20} cm^2)	Ω_6
ZnABCY	1.83	1.70	1.12
AlBCY	1.98	1.32	1.07
HfBL	2.73	1.35	0.98
ZrBL	2.75	1.09	0.98
GeBL	4.08	0.95	0.59
TeBL	4.23	0.83	0.74

Luminescence decay measurements were carried out with a pulsed dye laser (Spectra Physics Quanta Ray PDL-3), which was excited by the SHG light of a pulsed Nd:YAG (yttrium aluminum garnet) laser (Spectra Physics Quanta Ray GCR-11) and a gated integrator and a boxcar averager module (Stanford Research System model SR250). The lifetime of $^4H_4 \rightarrow {}^3H_6$ emission at 800 nm was determined by a least square fitting.

III. RESULTS AND DISCUSSION

A. Effects of composition on the Ω_t parameters

The Judd-Ofelt Ω_t intensity parameters of Tm^{3+} in the glasses are shown in Table II and Fig. 2. The value of Ω_2 in the tellurite glass is much larger than those in the present fluoride samples. There exists an increasing tendency of the Ω_2 parameter with the field strength of network former in the present samples. This may correlate with the increased asymmetry of ligand field of Tm^{3+} ion. We previously reported that in fluorophosphate glasses both the Ω_2 and quadrupole splitting of ^{151}Eu Mössbauer spectra increases with an increase of phosphate content.[12] These results are ascribed to the larger electric field gradient by divalent oxide ions than

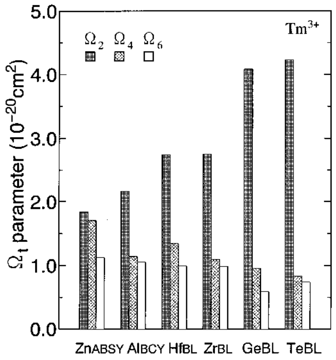

FIG. 2. Compositional variation of Ω_t parameters in glasses.

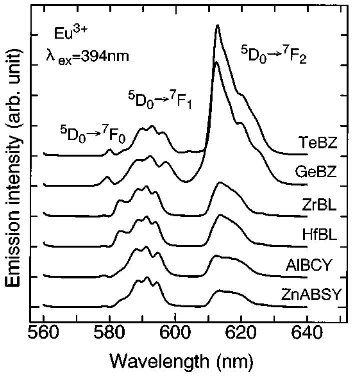

FIG. 3. Emission spectra of Eu^{3+} doped glasses.

that by monovalent fluoride ions and also to the covalency of the chemical bond between rare earth and ligand anions.

The Stokes fluorescence spectra of Eu^{3+}:$^5D_0\to{}^7F_{0-2}$ transitions in Eu^{3+} doped glasses with the same composition are shown in Fig. 3. The intensity ratio of ($^5D_0\to{}^7F_2$)/($^5D_0\to{}^7F_1$), R is much larger in oxide glasses than in fluoride glasses. Because the intensity of the denominator is independent of ligand field owing to the magnetic dipole nature and also because that of the numerator is proportional simply to the Ω_2 parameter, R should be a measure of Ω_2 parameter of rare earth ions in glass.[12,13] The R in Fig. 3 shows a similar tendency to that of Ω_2 parameter of Tm^{3+} ions in the corresponding glasses.

B. Effect of Ω_t parameters on the branching ratio of 0.36 and 0.45 μm emissions

The Tm^{3+} upconversion luminescence spectra of the glasses by 650 nm pumping are shown in Fig. 4. The ordinate of each spectrum is normalized by the intensity of the 450 nm band. The emission bands at 360, 450, and 480 nm can be assigned to $^1D_2\to{}^3H_6$, $^1D_2\to{}^3F_4$, and $^1G_4\to{}^3H_6$ transitions, respectively.[3,4] In the fluoride glasses, the intensity of 360 nm emission is comparable to that of the 450 nm emission. The relative intensity of 450 nm emission slightly increased in the order ZnABSY<AlBCY<ZrBL<HfBL<GeBZ<TeBZ. In the oxide glasses, the emission band of $^1D_2\to{}^3H_6$ near 360 nm is quite small.

Because the $\langle\|U^{(2)}\|\rangle^2$ of the $^1D_2\to{}^3F_4$ transition is large, the spontaneous emission probability, A, of the blue emission can be largely enhanced by the increased value of Ω_2, which reflects the asymmetry of ligand field.[8,12] A different A from $^1D_2$ level results in a different ratio of β, because the β from an initial $|bJ\rangle$ state to a terminal $|cJ'\rangle$ state can be defined as

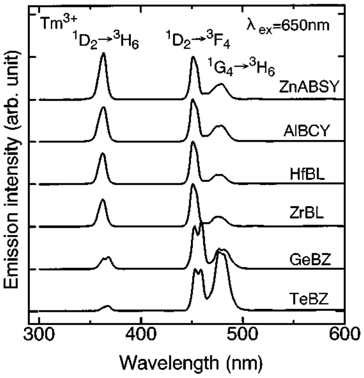

FIG. 4. Upconversion luminescence spectra of Tm^{3+} doped glasses by 650 nm pumping.

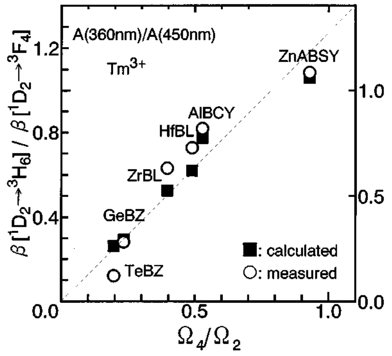

FIG. 5. Relation between measured and calculated intensity of uv and blue upconversions and Ω_4/Ω_2 ratio of Tm^{3+} ions.

$$\beta[bJ;cJ'] = \frac{A[bJ;cJ']}{\sum_{cJ'} A[bJ;cJ']}, \tag{3}$$

where $A[bJ;cJ']$ is the spontaneous emission probability given by[9]

$$A[bJ;cJ'] = \frac{64\pi^4 e^2}{3h(2J+1)\lambda^3} n \left[\frac{(n^2+2)^2}{9}\right] S[bJ:cJ']. \tag{4}$$

In this equation, $S[bJ:cJ']$ is obtained by Eq. (1). Thus the factors dominating the value of β's from $^1D_2$ to the lower states are the relative values of A, which are the functions of reduced matrix elements of each transition in Table I and also a set of Ω_t parameters of a given ligand field. Since the values of $\langle\|U^{(t)}\|\rangle^2$'s and λ^{-3} for the transition to other terminal states when $^3H_6$ and $^3F_4$ are negligibly small, the $\beta[{}^1D_2;{}^3F_4](=\beta_{45})$ and $\beta[{}^1D_2;{}^3H_6](=\beta_{36})$ are dominated approximately by the values of Ω_2 and Ω_4. The ratio β_{36}/β_{45} $[=A_{36}/A_{45}$ from Eq. (3)] obtained from the luminescence spectra and that calculated from Ω_t's for the present glasses are plotted as a function of Ω_4/Ω_2 ratio in Fig. 5 by open circles and closed squares, respectively. The measured β_{36}/β_{45} for the tellurite glass is a little lower than that calculated from Ω_t parameters. This is probably due to the intrinsic absorption edge of host glass around 400 nm, which makes the color of tellurite glasses yellowish.[14] However, as a whole, there is a good correlation between the measured and the calculated β_{36}/β_{45} ratios. Thus it can be concluded that we can control the branching ratio of uv and blue upconversions by designing the Ω_t parameters; a large β_{45} could be attained by selecting oxide hosts with a lower ligand field symmetry.

C. Luminescence lifetime and phonon sideband spectra

The phonon sideband (PSB) cannot be clearly observed for Tm^{3+} ion in glasses owing to the multiplet Stark splittings of its levels as well as inhomogeneous broadening of transition lines. Thus the measurement was done for the Eu^{3+}-doped glasses with the same composition instead. In

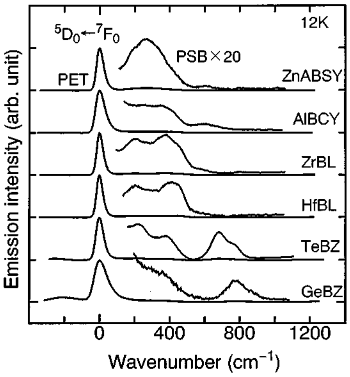

FIG. 6. Phonon sideband spectra of Eu^{3+} doped glasses.

the excitation spectra of Eu^{3+}:$^5D_0 \rightarrow {}^7F_2$ emission at 612 nm in Fig. 6, the PSB associated with the pure electronic $^5D_0 \leftarrow {}^7F_0$ transition[15] is multiplied by 20 times to study the phonon mode coupled with the rare earth ions. The observed phonon energy of the germanate (GeBL) glass is near 800 cm^{-1}, the highest, whereas that of the fluorozincate (ZnABSY) is near 300 cm^{-1}, the lowest among the present samples. The nonradiative loss due to multiphonon relaxation, which affects the radiative quantum efficiency and the excitation efficiency of the ESA, depends strongly on the phonon energy. The relationship among τ_f, radiative decay rate (=spontaneous emission probability, A) and nonradiative decay rate W_{NR} is given by

$$\tau_f^{-1} = \sum A + W_{NR} = \sum A + W_p + W_{ET}. \qquad (5)$$

In the case of an extremely low doping level (<0.3 mol %), the W_{ET} becomes negligibly small and thus the W_{NR} should be equal to W_p at 0.1 mol % TmF_3.[16] Because A is roughly proportional to a linear combination of Ω_t parameters, τ_f is dominated mainly by the value of W_p, which varies largely with the host. In Fig. 7 the obtained τ_f of $^3H_4$ level is plotted against the phonon energy, $\hbar\omega$ estimated from the PSB spectra in Fig. 6. We can see that τ_f decreases exponentially with an increase of $\hbar\omega$. This tendency can be explained approximately by the following relation for the multiphonon decay rate deduced by Miyakawa and Dexter:[17]

$$W_p = W_0 \exp(-\alpha \Delta E/\hbar\omega), \qquad (6)$$

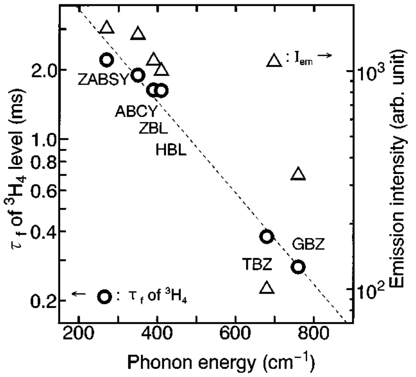

FIG. 7. Fluorescence lifetime of Tm^{3+}:$^3H_4$ level as a function of the phonon energy in the glass.

where the ΔE is the energy gap to the next lower level and α is a function of the electron-phonon interaction. Also the total intensity of two upconversion emissions observed by 100 mW pumping, I_{em} is plotted by an open triangle in the same figure. Apparently, both this intensity and τ_f of $^3H_4$, which is the intermediate excited level for $^1D_2$ upconversion (Fig. 1), show a similar tendency against $\hbar\omega$. The I_{em} of the TeBL glass is a little lower than the expected value, even lower than that of the GeBL glass. This can be ascribed to the self-absorption of the luminescences by the tellurite host matrix, which was discussed in the previous section. Therefore, we can conclude that the lower the multiphonon decay rate is, the more efficiently the upconversion emission is obtained.

IV. CONCLUSIONS

The branching ratio of $^1D_2 \rightarrow {}^3H_6$ (0.36 μm) and $^1D_2 \rightarrow {}^3F_4$ (0.45 μm) upconversion luminesnces of Tm^{3+} ions can be changed with the Judd-Ofelt Ω_t parameters, which depend on glass compositions. That of 0.45 μm blue emission increased with increasing Ω_2 value, which is a measure of asymmetry of Tm^{3+} ligand field. The intensity of 0.36 μm ultraviolet luminescence was largest in the fluorozincate glass with a low Ω_2/Ω_4 value. The control of branching ratio is possible by the ligand field design for Tm^{3+} ions in hosts.

---

[1] D. C. Hanna, R. M. Percival, I. R. Perry, R. G. Smart, J. E. Townsend, and A. C. Tropper, Opt. Commun. **78**, 187 (1990).

[2] J. Y. Allain, M. Monerie, and H. Poignant, Electron. Lett. **26**, 166 (1990).

[3] S. Tanabe, K. Hirao, and H. Toratani, Kotai-Butsuri (Solid State Phys.) **27**, 186 (1992).

[4] S. Tanabe, K. Tamai, K. Hirao, and N. Soga, Phys. Rev. B **47**, 2507 (1993).

[5] B. R. Judd, Phys. Rev. **127**, 750 (1962).

[6] G. S. Ofelt, J. Chem. Phys. **37**, 511 (1962).

[7] N. Spector, R. Reisfeld, and L. Boehm, Chem. Phys. Lett. **49**, 49 (1977).

[8] S. Tanabe, T. Ohyagi, N. Soga, and T. Hanada, Phys. Rev. B **46**, 3305 (1992).

[9] R. D. Peacock, *Structure and Bonding, Vol. 22* (Springer-Verlag, Berlin, 1975), p. 83.

[10] S. Tanabe, T. Ohyagi, S. Todoroki, T. Hanada, and N. Soga, J. Appl. Phys. **73**, 8451 (1993).

[11] S. Tanabe, T. Hanada, T. Ohyagi, and N. Soga, Phys. Rev. B **48**, 10 591 (1993).

[12] S. Tanabe, K.Hirao, and N. Soga, J. Non-Cryst. Solids **142**, 148 (1992).

[13] S. Tanabe, S. Yoshii, K. Hirao, and N. Soga, Phys. Rev. B **45**, 4620 (1992).

[14] S. Tanabe, K. Suzuki, N. Soga, and T. Hanada, J. Opt. Soc. Am. B **11**, 933 (1994).

[15] S. Tanabe and S. Todoroki, New Glass **7**, 189 (1992).

[16] S. Tanabe, in *Rare Earths*, edited by G. Adachi (The Rare Earth Society of Japan, Osaka, 1993), Vol. 23, p. 67.

[17] T. Miyakawa and D. L. Dexter, Phys. Rev. B **1**, 2961 (1970).